Shot noise in the leaky integrate-and-fire neuron

Nicolas Hohn*
Department of Otolaryngology, The University of Melbourne, 384-388 Albert Street, East Melbourne, Victoria 3002, Australia

Anthony N. Burkitt†
The Bionic Ear Institute, 384-388 Albert Street, East Melbourne, Victoria 3002, Australia

(Received 14 May 2000; revised manuscript received 8 September 2000; published 20 February 2001)

We study the influence of noise on the transmission of temporal information by a leaky integrate-and-fire neuron using the theory of shot noise. The model includes a finite number of synapses and has a membrane potential variance *de facto* modulated by the input signal. The phenomenon of stochastic resonance in spiking neurons is analytically exhibited using an inhomogeneous Poisson process model of the spike trains, and links with the traditional Ornstein-Uhlenbeck process obtained by a diffusion approximation are given. It is shown that the modulated membrane potential variance inherent to the model gives better signal processing capabilities than the diffusion approximation.

DOI: 10.1103/PhysRevE.63.031902 PACS number(s): 87.10.+e, 05.40.−a, 02.50.−r

I. INTRODUCTION

The presence of noise in a signal processing device is usually detrimental to performance. Sometimes, however, it can be beneficial as shown by the theory of stochastic resonance (SR). For a nonlinear system with periodic input, SR can be defined as an enhancement of the output signal-to-noise ratio (SNR) by the addition of noise [1].

Introduced two decades ago to explain the periodicity of the earth's ice ages [2], SR has been the subject of considerable interest over the last decade and has been demonstrated in various bistable systems [3,4] and living organisms [5,6]. Many studies involving peripheral sensory systems that have exhibited SR [7] have been carried out. SR has also been extended to monostable systems and in particular to excitable devices [8]. It has found a growing interest in neuroscience, since neural pathways contain many sources of noise and nonlinearities. Two sources of noise along a neural pathway are the channel noise due to random openings and closings of ion channels [9], and the synaptic noise or the so-called spontaneous activity due to uncorrelated spike trains [10]. There are a number of nonlinearities in the response of neurons to synaptic input, the most important being the thresholding mechanism for generating electrical spikes. The transmission of subthreshold stimuli by neurons has been studied using the FitzHugh-Nagumo model [11] and the leaky integrate-and-fire neuron model [12].

SR in a periodically driven leaky integrate-and-fire neuron model without a stimulus reset after firing has been analyzed recently [13,14]. However, these studies were carried out in the diffusion approximation [15,16] in which the number of synapses in the neuron is effectively infinite. The membrane potential dynamics is in this case described by a Langevin equation [17], corresponding to the limit of an infinite number of vanishingly small synaptic inputs. This approximation does not hold for neurons with a small number of afferent fibers as found, for example, in the auditory pathway. The aim of this paper is to study analytically and numerically the phenomenon of stochastic resonance in a leaky integrate-and-fire neuron receiving actual spike trains instead of a continuous waveform.

Analysis of SR in neurons transmitting spike trains is made difficult by the fact that the membrane potential is a right-continuous jump process, instead of a continuous process in the diffusion approximation. It was first studied in [18] with the input being the sum of a deterministic periodic spike train and a Poisson process representing the additive noise. With the choice of parameters in [18], the neuron was essentially acting as a coincidence detector, since two input spikes sufficiently close caused a threshold crossing. In [19], the addition of a deterministic spike train and a stochastic spike train formed the input of the neuron. A multipeak SNR was numerically exhibited for a particular correlation parameter of the stochastic spike train. However, this study was limited to the case where one spike of the noisy train was enough to generate a postsynaptic response. In another closely related study [20], the transmission of a large number of identical periodic spike trains with different phase shifts was shown to be enhanced by the addition of random Poisson spike trains. The neuron model in this study included the synaptic conductance, but only excitatory inputs were considered and the study was entirely numerical.

We investigate analytically and numerically the possible benefits of random firing patterns in a mathematically tractable neural model with a finite number of synapses. The spiking neuron model and a derivation of the membrane potential are presented in Sec. II. Statistics of the output spike train are analyzed in Sec. III. In Sec. IV, the phenomenon of SR in a spiking neuron is exhibited using the theory developed in the previous sections, and results are compared with those obtained from the diffusion approximation limit. Finally, in Sec. V, the main results are summarized and discussed.

*Corresponding author.
Email address: n.hohn@medoto.unimelb.edu.au
†Email address: a.burkitt@medoto.unimelb.edu.au

II. LEAKY INTEGRATE-AND-FIRE NEURON MODEL

A. The diffusion approximation

The stochastic leaky integrate-and-fire neuron will be used as a model of a nerve cell [21]. In this model, an input current charges the neuron membrane like a leaky capacitor with time constant τ. When the membrane potential reaches a threshold V_{th}, an output spike is fired and the membrane potential is deterministically reset. In between two firing events, the membrane potential of the neuron receiving infinitesimally small excitatory and inhibitory spikes from an infinite number of synapses is governed by the Itô-type stochastic differential equation [22]

$$dV(t)=\left(-\frac{V(t)}{\tau}+I(t)\right)dt+\sqrt{D}dW(t), \tag{1}$$

where $dW(t)$ is a standard Wiener process and $I(t)$ is the deterministic input current. After each threshold crossing, the membrane potential is reset to its resting potential $V_{res}=0$. In the rest of this paper, $I(t)$ is taken to be a positive periodic function with period T.

Assume that the membrane potential is v_0 at time t_0 and that the neuron does not fire between t_0 and t. The solution of the Langevin equation (1) is an Ornstein-Uhlenbeck (OU) process whose mean and variance can be obtained by using stochastic calculus rules [23] or by solving the corresponding Fokker-Planck equation [24]. They read, respectively,

$$\mathrm{E}[V(t)|v_0,t_0]=v_0e^{-(t-t_0)/\tau}+\int_{t_0}^{t}I(u)e^{(u-t)/\tau}du \tag{2}$$

and

$$\mathrm{Var}[V(t)|v_0,t_0]=\frac{D\tau}{2}(1-e^{-2(t-t_0)/\tau}). \tag{3}$$

Higher order cumulants are null [24]. The membrane potential therefore has a Gaussian distribution.

B. Finite-amplitude inputs

When the input spikes have a nonvanishing amplitude, the input spike trains are modeled by stochastic point processes, since it is the timing of spikes rather than their shape that conveys the information carried by the neuron [25]. A widely used description of the fluctuations of the neuron membrane potential between two firing events in this case is given by Stein's model [21],

$$dV(t)=-\frac{V(t)}{\tau}dt+a_edP_e(t)+a_idP_i(t), \tag{4}$$

where the resetting potential is set to 0. a_e and a_i are the respective amplitudes of incoming excitatory and inhibitory spikes. $P_e(t)$ and $P_i(t)$ are two inhomogeneous Poisson processes (IHPPs) with rates $\gamma_e(t)$ and $\gamma_i(t)$, describing the statistics of the excitatory and inhibitory input spike trains.

Equation (1) can be obtained from Eq. (4) by using a diffusion approximation [15,16]. As shown in [17], one way of deriving the OU diffusion process from Stein's equation is to take the limit $N\to\infty$ for the following quantities:

$$\gamma_e(t)=N\lambda_{in}(t)+\frac{N^2D}{2V_{th}^2},\quad \gamma_i(t)=\frac{N^2D}{2V_{th}^2}, \tag{5}$$

$$a_e=-a_i=\frac{V_{th}}{N},$$

where N is the number of synapses and $\lambda_{in}(t)$ is a T-periodic positive function. This requires that the input current $I(t)$ in Eq. (1) is defined as

$$I(t)=\lambda_{in}(t)V_{th}. \tag{6}$$

The membrane potential $V(t)$ is hence transformed from a right-continuous jump process solution of Eq. (4) to a fully continuous process solution of Eq. (1).

Equation (5) can be explained in biological terms as follows. Assume that the neuron receives input signals from N synapses and that each input transmits some information about a stimulus via excitatory spikes described by an inhomogeneous Poisson process with rate $\lambda_{in}(t)$. The resulting spike train at the soma is therefore an IHPP with rate $N\lambda_{in}(t)$. In the same time, the neuron receives uncorrelated excitatory and inhibitory spikes, described by a homogeneous Poisson process with rate $D/2V_{th}^2$, from N^2 synapses. The pooled inputs can be described by two IHPPs with rates $\gamma_e(t)$ and $\gamma_i(t)$. Moreover, in order for the input- and output-spike rates to be comparable, the postsynaptic potential amplitudes have to be of the order of V_{th}/N.

In the following, we will use Eq. (4) and Eq. (5) to derive the membrane statistics of a leaky integrate-and-fire neuron receiving excitatory and inhibitory spikes with small but nonvanishing amplitudes from a large but finite number N of synapses.

C. Membrane-potential statistics

A derivation of the membrane-potential probability density of a spiking neuron has already been published elsewhere [26]. A more compact version is sketched in the following for the particular case of Eq. (4) with the parameter values of Eq. (5). Assume that the membrane potential is v_0 at time t_0 and that the neuron does not fire between t_0 and t. Let $v_e(t)$ and $v_i(t)$ be the respective contributions of each IHPP train of impulses with rate $\gamma_e(t)$ and $\gamma_i(t)$. Since Eq. (4) is linear, its solution $V(t)$ can be obtained as $V(t)=v_e(t)+v_i(t)$. For instance, $v_e(t)$ can be seen as the output of a first-order low-pass linear filter with impulse response

$$f(t)=\begin{cases}e^{-t/\tau} & \text{if} \quad t\geqslant 0\\ 0 & \text{if} \quad t<0,\end{cases} \tag{7}$$

and input

$$d(t)=a_e\sum_k \delta(t-p_k), \tag{8}$$

where $\{p_k\}$ is a set of arrival times of an IHPP with rate $\gamma_e(t)$. Therefore $v_e(t)=a_e\Sigma_k f(t-p_k)$ is a shot noise process and its nth order cumulant is given by the generalized Campbell's theorem [27]:

$$l_e^{(n)}[v_e(t)|v_0,t_0]=a_e^n\int_{t_0}^{t}\gamma_e(u)[f(t-u)]^n du. \tag{9}$$

The same reasoning can be applied to $v_i(t)$. Since the inhibitory and excitatory spike trains are independent, $V(t)$ is a sum of two independent random variables $v_e(t)$ and $v_i(t)$, and its cumulants are obtained by summing the cumulants of $v_e(t)$ and $v_i(t)$. The expected value is the sum of two terms: the exponentially decaying initial value and the mean contribution of the incoming spikes in the time interval $[t_0,t]$,

$$\mathrm{E}[V(t)|v_0,t_0]=v_0e^{-(t-t_0)/\tau}+V_{th}\int_{t_0}^{t}\lambda_{in}(u)e^{(u-t)/\tau}du \tag{10}$$

and the variance reads

$$\mathrm{Var}[V(t)|v_0,t_0]=\frac{D\tau}{2}(1-e^{-2(t-t_0)/\tau})+\frac{V_{th}^2}{N}\int_{t_0}^{t}\lambda_{in}(u)e^{2(u-t)/\tau}du. \tag{11}$$

For $k>1$, higher order cumulants are

$$l^{(2k)}[V(t)|v_0,t_0]=\frac{D\tau V_{th}^{2k-2}}{2kN^{2k-2}}(1-e^{-2k(t-t_0)/\tau})+\frac{V_{th}^{2k}}{N^{2k-1}}\int_{t_0}^{t}\lambda_{in}(u)e^{2k(u-t)/\tau}du, \tag{12}$$

and

$$l^{(2k+1)}[V(t)|v_0,t_0]=\frac{V_{th}^{2k+1}}{N^{2k}}\int_{t_0}^{t}\lambda_{in}(u)e^{(2k+1)(u-t)/\tau}du. \tag{13}$$

As expected, taking the limit $N\to\infty$ gives a normal distribution solution of Eq. (1) with expected value and variance, respectively, given by Eqs. (2) and (3).

In the following, we focus on the case where the number N of incoming spike trains is large enough to assume that the membrane potential has a Gaussian distribution, but too small to approximate Eq. (11) by Eq. (3). The statistics of the membrane potential are therefore Gaussian with mean and variance, respectively, given by Eqs. (10) and (11). The variance of the membrane potential is therefore modulated by the input signal.

In the rest of this paper, the rate function of the input IHPP is modeled by a T-periodic sum of Gaussian functions [28],

$$\lambda_{in}(t)=r_{in}T\frac{1}{\sqrt{2\pi\eta_{in}^2}}\sum_{m=-\infty}^{+\infty}\exp\left(-\frac{(t-mT)^2}{2\eta_{in}^2}\right), \tag{14}$$

where r_{in} is the mean input rate and η_{in} is the standard deviation of the Gaussian functions. $r_{in}T$ is the average number of input spikes arriving at a synapse during one stimulus period T. The synchronization index, which measures the degree of phase locking between a spike train and a periodic stimulus [29,30], can be shown to be [28]

$$s_{in}=\exp\left[-2\left(\frac{\pi\eta_{in}}{T}\right)^2\right]. \tag{15}$$

The rate model of Eq. (14) was chosen for its ability to describe a spike train with an arbitrary synchronization index covering the full range (0,1), whereas a sinusoidal input rate function of the form $a(t)=a_0+2a_1\cos(\omega t+\phi)$ only describes spike trains with synchronization index $|a_1|/a_0$ in the range $[0,0.5]$ due to the positivity requirements of the rate function $a(t)$.

Figure 1 shows a plot of $\lambda_{in}(t)$, $V(t)$ and its theoretical variance for typical values of the input parameters. For low input synchronization indexes, $\lambda_{in}(t)$ is close to a sine function as shown in Fig. 1(a), where the solid curve represents $I(t)=\lambda_{in}(t)V_{th}$ as given in Eqs. (6) and (14). The dashed line represents the time-averaged input current. Figure 1(b) shows the values of the membrane potential in a typical simulation (black line), as well as the expected value Eq. (10) (thick gray line). As the model does not include reversal potentials, the membrane potential can theoretically diverge locally if the main source of input is the inhibitory spike train. However, in practice, the membrane potential is bounded and always depolarized by the input signal. Due to the fact that the second term of Eq. (11) proportional to $1/N$ is not neglected, the variance is modulated by the input signal. This is illustrated in Fig. 1(c).

D. Validity of the approximations

As shown previously, the probability density of the membrane potential can be approximated by a Gaussian by virtue of the central limit theorem. An upper bound of the error between the actual membrane potential distribution and the normal approximation can be obtained from the Berry-Esseen theorem [31]. However, in the particular case of a high-density shot noise process with parameters given by Eq. (5) and $D=0$, a result by [32] gives the following upper bound:

$$|F(x,t)-G(x)|<\frac{4}{3}\sqrt{\frac{2\pi}{NA_2(t)}}, \tag{16}$$

where $F(x,t)$ is the centered and normalized distribution function of the membrane potential, $G(x)$ is the error function, and $A_2(t)$ is given by

$$A_2(t)=e^{-2t/\tau}\int_{t_0}^{t}\lambda_{in}(u)e^{2u/\tau}du. \tag{17}$$

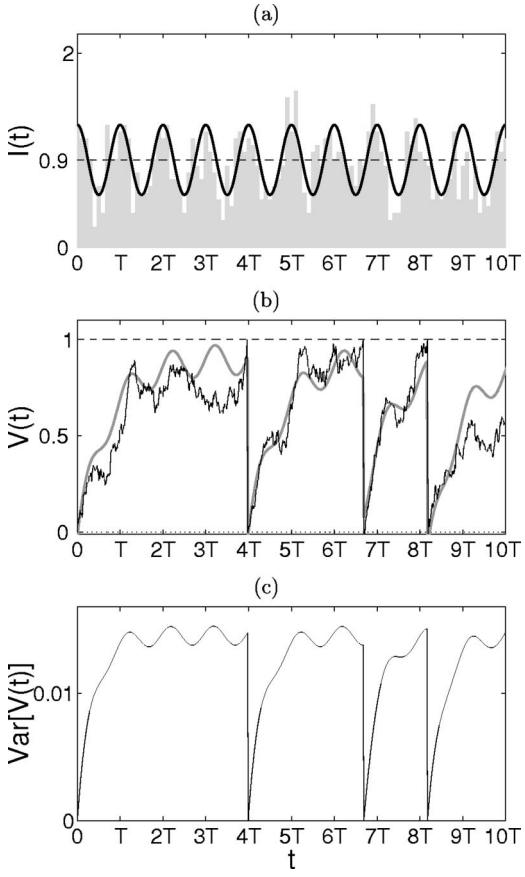

FIG. 1. (a) T-periodic input current $I(t)$ (solid line) and average input current (dashed line) as a function of time t for $\tau=1$, $T=1/0.7$, $s_{in}=0.2$, and $r_{in}=0.9$. The gray bar plot represents the input spike train with rate $N\lambda_{in}(t)$ and time bins $T/10$. (b) Typical simulated membrane potential (black line), theoretical expected value of the threshold-free membrane potential from Eq. (10) (thick gray line), threshold value (dashed line) and reseting value (doted line). (c) Theoretical variance of the threshold-free membrane potential from Eq. (11). For all the figures, voltages are given in units of the threshold V_{th}. Other parameters are $N=100$ and $D=0.02$.

As one would expect, the larger the number of input fibers N, the smaller the error made by the Gaussian approximation. The theoretical approximation was found to be in good agreement with computer simulations of Eq. (4) for $N>25$ over a large range of input parameters. The error scales as $1/\sqrt{N}$, as was previously found in a related study [28]. Figure 2 shows the simulated probability density of the membrane potential and the Gaussian approximation

$$g(x)=\frac{1}{\sqrt{2\pi\,\mathrm{Var}[V(t)|0,0]}}\exp\left(-\frac{\{x-\mathrm{E}[V(t)|0,0]\}^2}{2\,\mathrm{Var}[V(t)|0,0]}\right), \tag{18}$$

in the absence of a spike-generating threshold for $N=100$ input fibers, and for the noise values $D=0$ and $D=0.02$. The match between analytical approximation and computer simulation is very good.

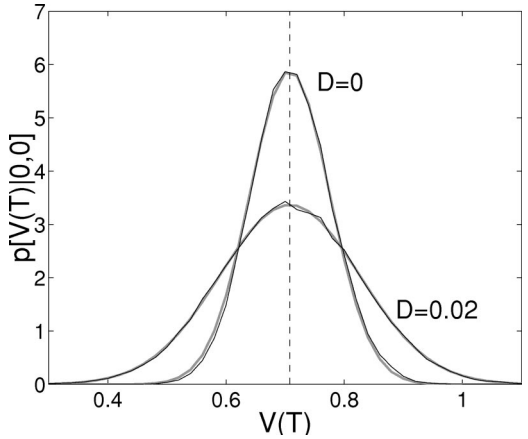

FIG. 2. Conditional probability density $p[V(T)|0,0]$ of the random variable $V(t)$ in the absence of a spike generating threshold at $t=T$ obtained from computer simulation of Eq. (4) (black) and analytical results from Eq. (18) (thick gray line) for $D=0$ (narrow bell-shaped curves) and $D=0.02$ (wide bell-shaped curves). The dotted line marks $E[V(T)|0,0]$, the conditional expected value of $V(T)$. Other parameters same as Fig. 1.

E. Noise

As the present paper is devoted to a study of stochastic resonance in neurons transmitting spike trains, the definition of the ''noise'' term is of primary importance.

When the membrane potential is described by the Langevin equation (1), the distinction between deterministic and stochastic inputs is obvious: the deterministic input is the current $I(t)$ and the noise term is clearly identified as the Wiener process $dW(t)$ with strength $\sqrt{D}$. After filtering, the noise term leads to the membrane-potential variance given by Eq. (3). In this case, the parameter $\sqrt{D}$ is the root-mean-square amplitude of the input noise. This quantity can then be normalized by the average distance to threshold [33] to characterize the noise in a stimulus-independent fashion. From Eq. (2), the time-averaged-offset expected value of the membrane potential is $\langle V_\infty\rangle$, defined as

$$\langle V_\infty\rangle=\frac{\tau}{T}\int_0^T I(t)dt. \tag{19}$$

The root-mean-square amplitude of the input noise is therefore given in normalized units by

$$\sigma=\frac{\sqrt{D\tau}}{V_{th}-\langle V_\infty\rangle}. \tag{20}$$

With this normalization process, the optimum noise level to be added to the input in the context of SR in a threshold detector is of the order of one in normalized units [33].

On the other hand, when using Eq. (4), both deterministic input information and noise are embedded in the same stochastic point process, making them less straightforward to separate than in the case of the Langevin equation (1). In a similar way to what was done in the previous paragraph, we can define the input noise in Eq. (4) from the membrane-potential variance. Following the decomposition of

$\mathrm{Var}[V(t)|v_0,t_0]$ into two terms in Eq. (11), the input noise is expressed as the sum of two independent random variables representing, respectively, the noise due to the spontaneous activity with root-mean-square amplitude $\sqrt{D\tau}$, and the noise due to the finite number of synapses with root-mean-square amplitude $\sqrt{\tau r_{in} V_{th}^2/N}$. In this case, the time-averaged-offset expected value of the membrane potential reads

$$\langle V_\infty \rangle = \frac{\tau V_{th}}{T} \int_0^T \lambda_{in}(t)dt = \tau r_{in} V_{th}, \tag{21}$$

which gives $\langle V_\infty \rangle = r_{in}$ with the choice of units $\tau = 1$, $V_{th} = 1$ as in Fig. 1. The normalized input noise root-mean-square amplitude can therefore be defined as

$$\sigma = \sqrt{\sigma_N^2 + \sigma_D^2}, \tag{22}$$

where

$$\sigma_N = \frac{1}{V_{th} - \langle V_\infty \rangle} \sqrt{\frac{\tau r_{in} V_{th}^2}{N}} = \frac{1}{1 - \tau r_{in}} \sqrt{\frac{\tau r_{in}}{N}}, \tag{23}$$

and

$$\sigma_D = \frac{\sqrt{D\tau}}{V_{th} - \langle V_\infty \rangle} = \frac{\sqrt{D\tau}}{V_{th}(1 - \tau r_{in})}. \tag{24}$$

In the following, σ_N will be referred to as ''internal'' shot noise since it is due to a parameter internal to the system, namely, the finite number N of synapses. σ_D will be called ''external'' diffusive noise as it is the noise quantity already present in the limit of vanishingly small inputs and does not depend on the neuron intrinsic parameters. This external noise can be modeled as the spontaneous activity received by the neuron, i.e., activity not correlated to the stimulus. In the limit $N \to \infty$, Eq. (22) becomes $\sigma = \sigma_D$ since $\sigma_N = 0$.

III. OUTPUT STATISTICS

In this section, we examine the statistical properties of the neuron output. The first-passage time density (FPTD) $\rho(t)$, which is equivalent to the interspike interval density, can be derived from the conditional probability density of the membrane potential by solving an integral equation [24,34] and finding the eigenfunction corresponding to eigenvalue 1 of an asymptotically stable Markov operator representing the spiking phase transition density [13,14]. The output phase density $h(\theta)$, mean firing rate r_{out}, and synchronization index s_{out} can be derived from the first-passage time density in a straightforward way. As shown in Fig. 3, the agreement between analytical and computer simulated FPTDs is very good. We first consider the case of a time-homogeneous input in Sec. III A in order to understand the basic internal mechanism of a single neuron and to study the consequences of superposing output spike trains. In Sec. III B, we extend the results to a time-inhomogeneous input.

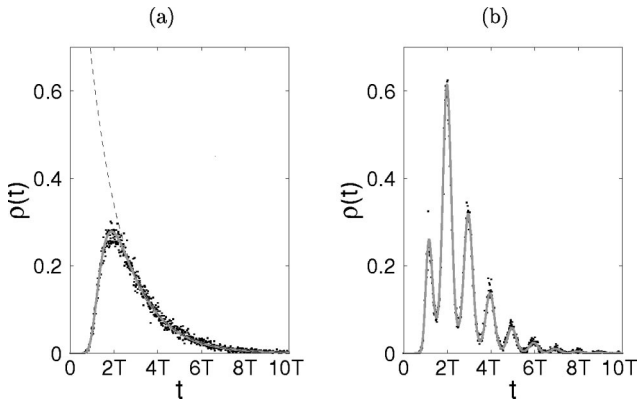

FIG. 3. Interspike interval histogram obtained from computer simulations of 50 000 output spikes (dots) and theoretical FPTD $\rho(t)$ (gray line) for (a) $s_{in} = 0$ and (b) $s_{in} = 0.2$. Other parameters are the same as as Fig. 1. Exponential fit to the FPTD in the case of a time-homogeneous input is shown by the dotted line.

A. Time-homogeneous input

When the input is a homogeneous Poisson process, the output spike train is a stationary renewal process and all the information about the spike train is contained in the FPTD. As shown by the exponential fit in Fig. 3(a), the output spike train can be well approximated by a dead-time Poisson process. The power-spectrum density of the output spike train can be obtained from the FPTD as [35,34]

$$P(f) = \frac{1}{\langle t \rangle} \left(1 + \frac{\tilde{\rho}(f)}{1 - \tilde{\rho}(f)} + \frac{\tilde{\rho}(-f)}{1 - \tilde{\rho}(-f)} \right), \tag{25}$$

where $\tilde{\rho}(f)$ is the Fourier transform of $\rho(t)$ and $\langle t \rangle$ is the mean firing time. An example of power-spectrum densities obtained from Eq. (25) and from computer simulations of Eq. (4) is shown in Fig. 4(a). The power spectrum is flat except for a dip at low frequencies, in accordance with the almost Poissonian nature of the output spike train exhibited by the exponential fit in Fig. 3(a). In fact, as the input is uncorrelated, the deviation of the output spike train from a Poisson process is due to internal characteristics of the neuron that can be described as follows. The neuron can theoretically fire at any time after the last firing event with a nonzero probability [36], since refractory effects are ignored here. However, the probability of having two output spikes fire in a very small time interval is extremely low due to the deterministic reset of the membrane potential after a firing event and the subsequent time taken by the membrane potential to reach its mean depolarization value $\langle V_\infty \rangle$. The model therefore has a pseudorefractory period, as indicated by the nearzero probability density of having short interspike intervals, which is illustrated in Fig. 3(a). The dip at low frequencies in the simulated power spectrum is consistent with such a pseudorefractory period [37]. The simulated power spectrum was obtained by discrete Fourier transformation of the simulated output spike train using a periodogram estimate [38] and a rectangular window to allow for

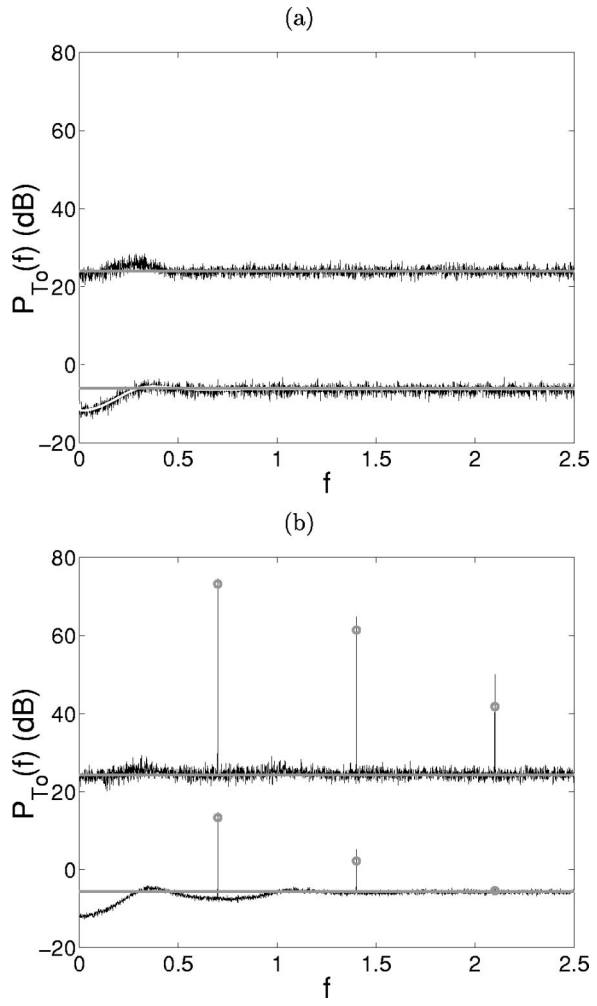

FIG. 4. (a) Power-spectral density of a single output spike train (bottom) and of the superposition of 1000 output spike trains (top) obtained from computer simulation of Eq. (4) (black), Poisson approximation as defined by Eq. (30) (thick straight gray line), and theoretical result from Eq. (25) (white line) in the case of a homogeneous input $s_{in}=0$. (b) Same as for (a) with inhomogeneous input $s_{in}=0.2$. The thick gray line and circles represent the first-order approximation of, respectively, the background power spectrum and its values at integer multiples of the driving frequency, as described by Eq. (30). Observation time $T_0=1000$. Other parameters are the same as Fig. 1. Frequency f in units of $1/\tau$.

an easy comparison with theoretical results.

Since the sum of independent renewal processes tends to a Poisson process [35], the superposition of a large number of output spike trains can be approximated by a homogeneous Poisson process. As can be seen in Fig. 4(a), which shows the power spectral densities for a homogeneous input, the power spectrum of the superposed output spike trains is fairly flat, in agreement with a Poisson process. As the dip at low frequencies due to the pseudorefractory period vanishes, the effects of the reset of the membrane potential after the firing of each individual neuron can be neglected when looking at the response of a large number of neurons. The resulting spike train can be described by a homogeneous Poisson process with a firing rate that is the sum of each individual firing rate.

B. Inhomogeneous input

When the input spike trains do not form a homogeneous process, the output spike train is not a renewal process and Eq. (25) does not hold. We will focus in the following on periodic inputs. Recently developed techniques can be used to get the exact power spectrum density in this case [36]. However, this exact calculation of a power spectrum is highly computational and not well suited for the numerous successive evaluations required for a study of stochastic resonance. Another alternative consists in computing the exact value of the power spectrum at integer multiples of the driving frequency [13] and approximating the rest of the spectrum by a flat Poissonian background [39]. This approximation is not very accurate at low frequencies due to the pseudorefractory period of the neuron and the dip in the power spectrum, a phenomemon largely independent of the exact nature of the spike train.

If one considers the pooled outputs of a large number of neurons, the resulting spike train can be approximated by an IHPP with time dependent rate [35]. This was shown in [40] by time demodulating the FPTD of the superposed spike trains to obtain a time-homogeneous process and applying statistical tests to compare the resulting FPTD with an exponential function. In the present study, we focus on the resulting power spectrum rather than the FPTD, since the SNR is obtained from the former quantity. From [40], it is possible to get the output statistics of the pooled spike train from those of a single unit. Assume that the pooled output spike train can be described by an IHPP with rate $\Gamma(t)$. We can rewrite $\Gamma(t)$ as $\Gamma(t)=N\alpha(t)$ to show that the pooled output is the sum of N spike trains with analogue statistics. This is equivalent to considering the output spike train of a single unit as an IHPP with rate $\alpha(t)$. Even if this is clearly incorrect due to the pseudorefractory effects of the model, it is an acceptable approximation since the pooled output is an IHPP.

It can be shown that an inhomogeneous Poisson train of impulses with rate $\alpha(t)$ has an autocorrelation function $R(t,\epsilon)=\alpha(t)\alpha(t+\epsilon)+\alpha(t)\delta(\epsilon)$ [41]. If $\alpha(t)$ is periodic, the process is periodically correlated or second-order cyclostationary [42]. SR for cyclostationary processes has recently been studied in threshold devices [43] using a two-dimensional Fourier transform of the signal covariance. In the following, we shall use a stationarized version of the autocorrelation function obtained by a time average over one period of the input stimulus [18] or by imposing a uniform distribution of the phase of the inhomogeneous rate of input on the initial condition [44]. Using a Fourier series expansion of the periodic rate $\alpha(t)$, the phase-averaged autocorrelation function reads

$$\begin{aligned}\langle R(t,\epsilon)\rangle &= \langle \alpha(t)\alpha(t+\epsilon)+\alpha(t)\delta(\epsilon)\rangle \\ &= \alpha_0^2+\frac{1}{2}\sum_{k=1}^{\infty}|\alpha_k|^2\cos\left(k\frac{2\pi}{T}\epsilon\right)+\alpha_0\delta(\epsilon),\end{aligned} \tag{26}$$

where $\langle\rangle$ denotes a phase average and

$$\alpha_k = \frac{1}{T}\int_T \alpha(t)\exp\left(-jk\frac{2\pi}{T}t\right)dt. \tag{27}$$

The stationary power spectrum of the spike train over a finite duration T_0 is defined as [38]

$$P_{T_0}(\omega) = \frac{1}{T_0}\left|\int_0^{T_0}\langle R(t,\epsilon)\rangle e^{-j\omega\epsilon}d\epsilon\right|. \tag{28}$$

$P_{T_0}(\omega)$ consists of a flat background with intensity α_0 giving the average firing rate, and peaks at integer multiples of the input frequency resulting from the periodicity of $\alpha(t)$.

As stated in the Introduction, SR will be exhibited by studying the variations of the output SNR as a function of the input noise. The SNR is defined as the ratio between the amplitude of the power spectrum at the driving frequency and the noise background. Using Eqs. (26) and (28), it can be approximated by

$$R_{T_0} = 10\log_{10}\left(\frac{|\alpha_1|^2 T_0}{2\alpha_0}\right) = 10\log_{10}\left(\frac{r_{out}s_{out}^2 T_0}{2}\right), \tag{29}$$

where $s_{out} = |\alpha_1|/\alpha_0$ is the synchronization index of the output spike train and $r_{out} = \alpha_0$ is its average firing rate. A similar expression was derived for the SNR of an inhomogeneous Poisson train of pulses in [8] and used in [40] for an infinite time window. The assumption of an infinite time window is not biologically realistic as the neuron has to process the information in a finite time [39], and it is also not well suited for comparison with computer simulations.

From Eq. (29), the SNR is a first-order quantity that only depends on the first two Fourier coefficients (α_0, α_1) of the rate $\alpha(t)$. Therefore, any rate function with the first two Fourier coefficients given, respectively, by α_0 and α_1 will define an IHPP with the same average firing rate and SNR as the actual output spike train. We model in this study the output rate function *a priori* by $\lambda_{out}(t)$ the T-periodic sum of Gaussian functions defined by Eq. (14), using the subscript ''out'' to specify the output spike train. The calculation of the output synchronization index and mean firing rate of a single unit allows the parameters r_{out} and η_{out} in Eq. (14) to be uniquely defined. Hence, $\lambda_{out}(t)$ is a first-order approximation of the actual output rate $\alpha(t)$. The first-order approximation of the output power spectrum becomes

$$P_{T_0}^{(1)}(\omega) = \frac{1}{T_0}\left|\int_0^{T_0}\langle R^{(1)}(t,\epsilon)\rangle e^{-j\omega\epsilon}d\epsilon\right|, \tag{30}$$

with

$$R^{(1)}(t,\epsilon) = \lambda_{out}(t)\lambda_{out}(t+\epsilon) + \lambda_{out}(t)\,\delta(\epsilon). \tag{31}$$

As seen in Fig. 4(b), $P_{T_0}^{(1)}(\omega)$ gives the same value as the simulations for the background noise and at the driving frequency, and therefore the same SNR. However, values of $P_{T_0}^{(1)}(\omega)$ at higher integer multiples of the driving frequency are not reliable as they explicitly depend on higher order terms of the Fourier series of the output rate $\alpha(t)$. They are nevertheless relatively close to the simulations results. This can be explained by looking at the spiking phase transition density $h(\theta)$. $h(\theta)$ and the output rate $\alpha(t)$ are linked by the equation [13,14,45]

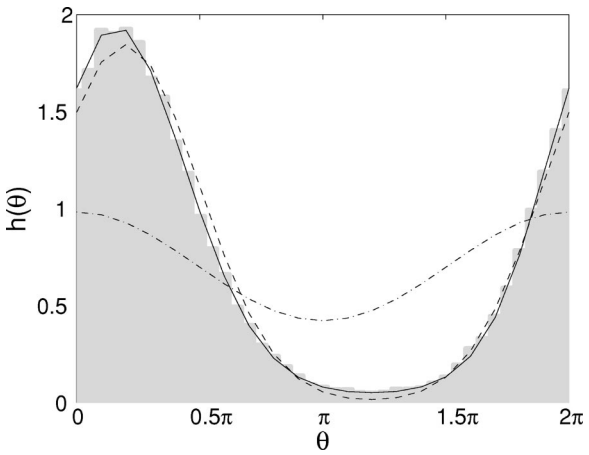

FIG. 5. Spiking phase distribution of the input spike train (dash-dotted) and the output spike train of a single unit obtained from the theory $h(\theta)$ (solid) given by Eq. (32) and from the first-order approximation $h^{(1)}(\theta)$ from Eq. (33) (dashed). The gray bar plot is obtained from simulation of 50 000 output spikes. Same parameters as Fig. 1.

$$h(\theta) = \frac{1}{r_{out}T}\alpha\left(\frac{T\theta}{2\pi}\right), \quad 0 \leqslant \theta \leqslant 2\pi. \tag{32}$$

It can be approximated up to the first order by

$$h^{(1)}(\theta) = \frac{1}{r_{out}T}\lambda_{out}\left(\frac{T\theta}{2\pi}\right), \quad 0 \leqslant \theta \leqslant 2\pi. \tag{33}$$

As shown in Fig. 5, in which the spiking phase distribution is plotted for both the input and output spike trains, $h(\theta)$ is a smooth function with a single maximum for a large range of input parameters, and is therefore well approximated by Eq. (33). The main advantage of using λ_{out} and $h^{(1)}(\theta)$ instead of the exact parameters $\alpha(t)$ and $h(\theta)$ is that the former are analytically accessible whereas the later can only be numerically computed.

IV. STOCHASTIC RESONANCE

Having introduced the neuron model and its output statistics in the previous sections, we may now study the phenomenon of SR from an analytical point of view in a neuron that transmits spike trains, instead of the numerical approach taken in earlier studies [19,20].

As defined in Sec. II E, there are two sources of noise in the neuron model: an ''internal'' shot noise due to a finite number N of input fibers and characterized by σ_N, and an ''external'' diffusive noise modeling the spontaneous neural activity and characterized by σ_D. We will look in the following at the influence of the diffusive noise for a given neuron architecture specified by a fixed N. When a deterministic signal and an additive noise are the inputs of a threshold

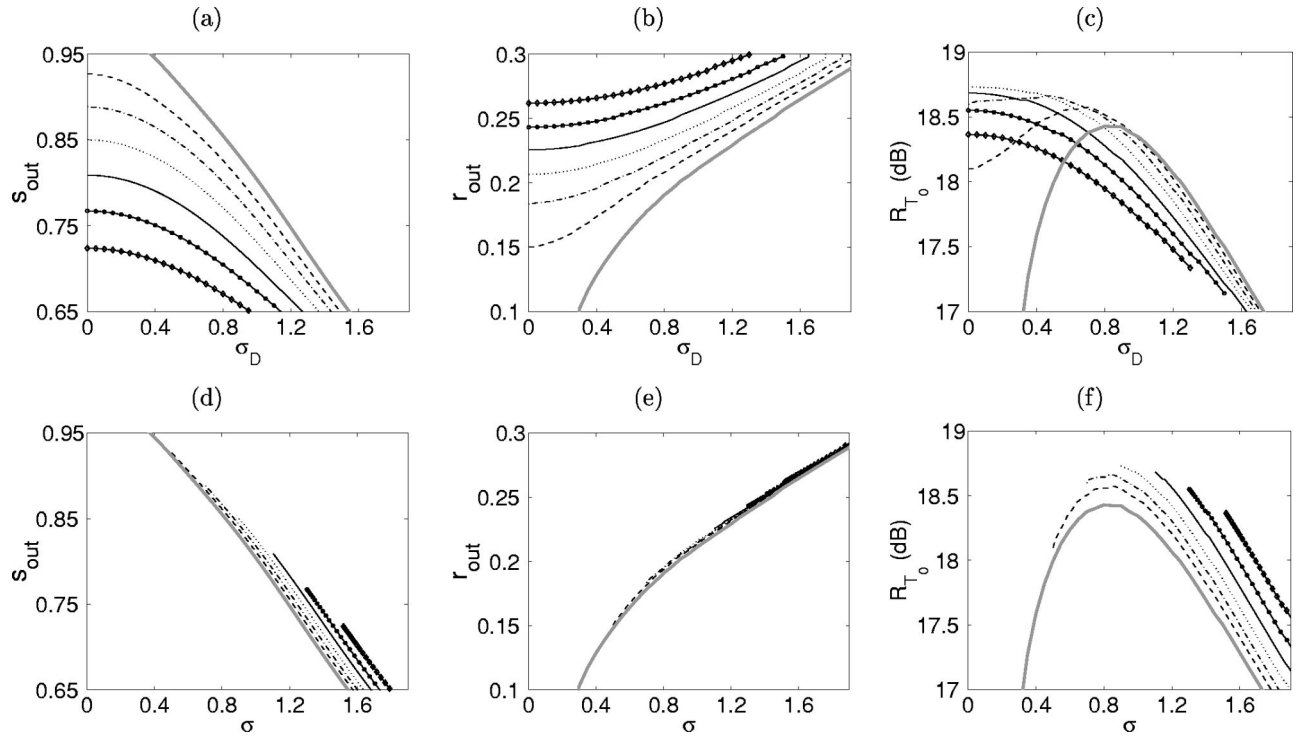

FIG. 6. Upper row: (a) Output synchronization index s_{out}, (b) output mean firing rate r_{out}, and (c) output SNR R_{T_0} as a function of the normalized spontaneous activity σ_D. Lower row: (d) s_{out}, (e) r_{out}, and (f) R_{T_0} as a function of the total normalized noise σ. Input parameters: $T=1/0.7$, $s_{in}=0.2$, $\langle V_\infty \rangle = r_{in}=0.9$, and $T_0=1000$ with units $\tau=1$, $V_{th}=1$. Results for the diffusion approximation (solid gray line) and for the values of N corresponding to $\sigma_N=0.5$ (dashed), $\sigma_N=0.7$ (dashdot), $\sigma_N=0.9$ (dotted), $\sigma_N=1.1$ (solid), $\sigma_N=1.3$ (circles), and $\sigma_N=1.5$ (diamonds).

device, a necessary condition to exhibit SR is that the deterministic input is too weak to cross the threshold alone [8]. As deterministic and stochastic inputs cannot be separated in Eq. (4), this condition is approximated here by requiring that the expected value of the membrane potential be subthreshold. We first briefly review the case of the diffusion approximation to set a benchmark with which our results will be compared.

A. Diffusion approximation

In the diffusion approximation, the number of input fibers is effectively infinite ($N\to\infty$) and the results of stochastic resonance in sensory neurons apply [13,14]. When no spontaneous activity is added to the neuron, i.e., $D=0$, the neuron cannot fire since the input signal always remains subthreshold. As the value of D is increased, the threshold is likely to be first crossed at a local maximum of the membrane potential, but the neuron can skip a large number of periods between successive firing events. The output synchronization index is therefore high, whereas the output firing rate is low. The more noise, the higher the firing rate at the expense of a less synchronized output train. The maximum SNR is obtained as a trade off between the output synchronization index and the firing rate. The output synchronization index, the mean firing rate, and the SNR for the diffusion approximation are given as a function of σ_D in Figs. 6(a)–6(c) and as a function of σ in Figs. 6(d)–6(f). As $\sigma=\sigma_D$ in the diffusion approximation, these curves (thick gray lines) are similar on the two noise scales, and will be used as a reference to study the influence of the number of synapses in the next section.

B. Finite number of fibers

Having a finite number of input fibers modifies the above picture. Indeed as seen from Eq. (11), even in the absence of spontaneous activity, i.e., $D=0$, the membrane potential has a nonzero variance due to the finite number N of input fibers, and threshold crossings are therefore possible. Thus depending on the value of N, the intrinsic noise level characterized by σ_N might be smaller or larger than the optimum noise level σ_{opt}. As the phenomenon of SR in a threshold device is observed for an input noise with standard deviation of the order of the mean distance to threshold [33], the normalized standard deviation σ_{opt} is of order one. For $\sigma_N<\sigma_{opt}$, the addition of an increasing amount of spontaneous activity to the system will cause it to exhibit the phenomenon of SR as the SNR will first increase until $\sigma_N^2+\sigma_D^2=\sigma_{opt}^2$, and then decrease as σ_D increases further. On the other hand, for $\sigma_N>\sigma_{opt}$, the addition of spontaneous activity will only deteriorate the performance of the system and the SNR will decrease. The synchronization index and mean firing rate as a function of σ_D are, respectively, plotted for different values of σ_N in Figs. 6(a) and 6(b). The resulting SNR from Eq. (29) is plotted in Fig. 6(c).

For a given σ, the output synchronization index is largest for the smallest number of input fibers available as shown in

Fig. 6(d). In contrast, the average firing rate remains almost independent of the noise modulations, since it is only related to the average noise contribution to the system. This fact is illustrated in Fig. 6(e). For a given noise strength σ, the largest SNR is therefore obtained for the sum $\sigma_D^2+\sigma_N^2$ with the largest possible σ_N, i.e., the smallest available number of input fibers.

C. The benefit of noise modulation

An interesting finding of this study is that for a given average noise level, having a membrane-potential variance modulated by the input signal gives a SNR slightly larger than the one obtained in the diffusion approximation with the same average noise level. The observations from the previous paragraph can be explained as follows.

It can be seen from Eq. (11) that there exists a phase delay between the expected value and the variance of the membrane potential, which is a function of the input frequency. However, as it can be shown to be less than $\pi/9$, the relative influence of the input frequency on the enhancement of the SNR by noise modulation has been neglected in this study. Thus, as the noise modulation increases, there is more and more noise near the local maxima of the average membrane potential, and less noise near the local minima. The threshold crossings are therefore more likely to occur near the local maxima of the average membrane potential, while crossings at other phase values are less likely to occur. The output spike train will therefore be better synchronized to the input stimulus than an output spike train obtained for a larger number of input fibers [Fig. 6(d)] while the average rate of firing remains the same [Fig. 6(e)]. The SNR of the output spike train is thus enhanced [Fig. 6(f)].

This result can be related to the observation of an earlier study [46], where it was shown that aperiodic SR could be enhanced by modulating the noise strength, either by the membrane potential or by the threshold crossing rate. However, in the present study this phenomenon appears as a natural consequence of having a finite number of synapses in the neuron model without any of the artificial mechanisms used in [46]. Qualitatively similar results were obtained in a numerical study of aperiodic SR in a FitzHugh-Nagumo neuron model with white and correlated additive noise [47].

As shown in Fig. 6(f), noise modulation improves the performance of the system in the sense that if a certain noise intensity σ is allocated to the neuron, a modulated noise will give a higher SNR than an unmodulated noise with the same intensity. Figure 7 shows the conditional variance of the membrane potential for the noise level $\sigma=0.9$, obtained first as $\sigma=\sigma_D=0.9$, corresponding to the diffusion approximation case (thick gray line), and as $\sigma=\sigma_N=0.9$, corresponding to the maximum achievable SNR. Therefore, there exists an optimum neuron architecture, described in the present case by $N=111$ input fibers, that best transmits a given stimulus, specified here by $T=1/0.7$, $\langle V_\infty\rangle=0.9$, and $s_{in}=0.2$ (with units $\tau=1$, $V_{th}=1$). Figure 8 shows the maximum SNR that can be achieved as a function of the noise intensity σ. It is the envelope of the set of curves plotted in Fig. 6(f) obtained by keeping σ_N as large as possible. The

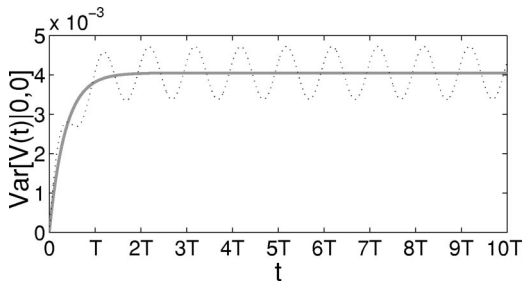

FIG. 7. Membrane-potential variance for $\sigma=0.9$, plotted for the diffusion approximation case $\sigma_D=0.9$ (solid gray line) and for the case $\sigma_N=0.9$ corresponding to the maximum SNR (dotted line).

SNR in the diffusion approximation is given as a reference (thick gray line). For small values of σ, the two curves are similar since σ_N is too small to create any noticeable noise modulation. As σ increases, the value of σ_N can be increased and the noise modulation is more and more pronounced with the effect of enhancing the SNR. It is interesting to notice that the noise modulation does not change the location of the maximum SNR, only its value.

V. CONCLUSION

This study has established the phenomenon of stochastic resonance in leaky integrate-and-fire neurons that transmit spike trains without a stimulus reset after firing in a fully systematic way by using the theories of inhomogeneous Poisson processes and shot noise. Since both input and output spike trains are modeled in the same way, the method is consistent and can be extended to a succession of neurons along a neural pathway. When the number of input fibers is finite, it has been proven that the stochastic jump process representing the membrane potential has a Gaussian distribution for which the mean and variance are given. As this distribution is relatively close to the one of the traditional diffusion approximation, results concerning the frequency tuning of neurons by means of the noise [48,33] are expected to also be valid for the model presented in this study.

The main result to come out of this study is that it is

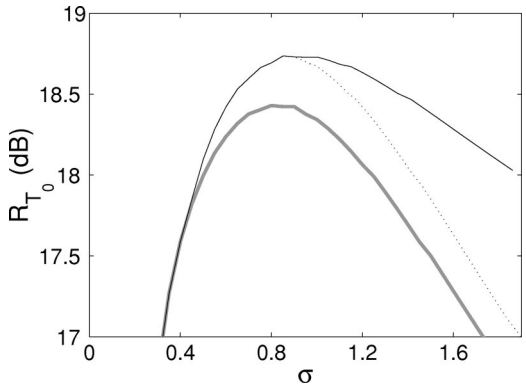

FIG. 8. Optimum SNR (solid black line) as a function of σ. SNR obtained for the diffusion approximation (thick gray line). SNR curve reaching the maximum SNR obtained for $\sigma_N=0.9$ (dotted line).

worth investigating the signal processing properties of neurons with a large but finite number of input fibers, as they have the interesting properties of having a membrane potential variance *de facto* modulated by the input stimulus. In the framework of SR, this allows for an output SNR larger than what would be obtained with an infinite number of input fibers and the same average input noise. This is achieved by allocating the noise where it is most needed to cross the threshold, i.e., near local maxima of the membrane-potential expected value, while reducing it where it will be less useful, namely, around local minima of the expected value of the membrane potential. By comparison, the noise is uniformly allocated in the diffusion approximation limit leading to lower performances.

Another result of this study concerns a qualitative justification of using simple threshold detector devices as neuron models in large arrays of neurons in parallel. Starting from the simple but still biologically realistic leaky integrate-and-fire neuron model, we have given qualitative arguments for neglecting the membrane reset after firing in neuron ensembles, and therefore the use of even simpler neuron models such as threshold detectors may be justified.

In conclusion, it appears theoretically possible to enhance the information transfer along a neural pathway such as the auditory pathway by adding a noisy component to the input signal. Being a direct consequence of a thresholding mechanism, SR in neurons is highly dependent on the threshold level; and analytical studies of large arrays of neurons in parallel with the same input signal, independent noise sources, and different thresholds will have to be carried out to gain a better understanding of the phenomenon.

ACKNOWLEDGMENTS

N.H. was partly supported by Bourses Région Rhône Alpes de Formation à l'Etranger. A.N.B. was funded by the Cooperative Research Center for Cochlear Implants, Speech and Hearing Research and The Bionic Ear Institute. We would like to thank H. E. Plesser for critically reading an earlier version of the manuscript.

[1] L. Gammaitoni, P. Hänggi, P. Jung, and F. Marchesoni, Rev. Mod. Phys. **70**, 223 (1998).
[2] R. Benzi, A. Sutera, and A. Vulpiani, J. Phys. A **14**, L453 (1981).
[3] S. Fauve and F. Heslot, Phys. Lett. **97A**, 5 (1983).
[4] B. McNamara and K. Wiesenfeld, Phys. Rev. A **39**, 4854 (1989).
[5] J. K. Douglas, L. Wilkens, E. Pantazelou, and F. Moss, Nature (London) **365**, 337 (1993).
[6] J. E. Levin and J. P. Miller, Nature (London) **380**, 165 (1996).
[7] K. Wiesenfeld and F. Moss, Nature (London) **373**, 33 (1995).
[8] K. Wiesenfeld *et al.*, Phys. Rev. Lett. **72**, 2125 (1994).
[9] J. A. White, J. T. Rubinstein, and A. R. Kay, Trends Neurosci. **23**, 131 (2000).
[10] H. C. Tuckwell, *Introduction to Theoretical Neurobiology: Volume 2, Nonlinear and Stochastic Theories* (Cambridge University Press, Cambridge, 1988).
[11] A. Longtin, J. Stat. Phys. **70**, 309 (1993).
[12] A. R. Bulsara *et al.*, Phys. Rev. E **53**, 3958 (1996).
[13] H. E. Plesser and T. Geisel, Phys. Rev. E **59**, 7008 (1999).
[14] T. Shimokawa, K. Pakdaman, and S. Sato, Phys. Rev. E **59**, 3427 (1999).
[15] L. M. Ricciardi, Biol. Cybern. **24**, 237 (1976).
[16] P. Lánský, J. Theor. Biol. **107**, 631 (1984).
[17] P. Lánský, Phys. Rev. E **55**, 2040 (1997).
[18] F. Chapeau-Blondeau, X. Godivier, and N. Chambet, Phys. Rev. E **53**, 1273 (1996).
[19] G. Mato, Phys. Rev. E **58**, 876 (1998).
[20] X. Godivier and F. Chapeau-Blondeau, Europhys. Lett. **35**, 473 (1996).
[21] R. B. Stein, Biophys. J. **5**, 173 (1965).
[22] L. M. Ricciardi, *Diffusion Processes and Related Topics in Biology*, Lecture Notes in Biomathematics Vol. 14 (Springer Verlag, Berlin, 1977).
[23] A. Lasota and M. C. Mackey, *Chaos, Fractals and Noise: Stochastic Aspects of Dynamics*, 2nd. ed., Applied Mathematical Sciences Vol. 97 (Springer-Verlag, New York, 1994).
[24] N. van Kampen, *Stochastic Processes in Physics and Chemistry*, 2nd ed. (North Holland, Amsterdam, 1992).
[25] G. L. Gerstein and B. Mandelbrot, Biophys. J. **4**, 41 (1964).
[26] A. N. Burkitt and G. M. Clark, Neural Comput. **11**, 871 (1999).
[27] A. Blanc-Lapierre and R. Fortet, *Théorie Des Fonctions Aléatoires* (Masson, Paris, 1953).
[28] R. Kempter, W. Gerstner, J. L. van Hemmen, and H. Wagner, Neural Comput. **10**, 1987 (1998).
[29] J. M. Goldberg and P. B. Brown, J. Neurophysiol. **32**, 613 (1969).
[30] D. H. Johnson, J. Acoust. Soc. Am. **68**, 1115 (1980).
[31] V. V. Senatov, *Normal Approximation: New Results, Methods and Problems*, *Modern Probability and Statistics* (VSP, The Netherlands, 1998).
[32] A. Papoulis, J. Appl. Probab. **8**, 118 (1971).
[33] H. E. Plesser and T. Geissel, Neurocomputing (to be published).
[34] H. E. Plesser and S. Tanaka, Phys. Lett. A **225**, 228 (1997).
[35] D. Cox and H. Miller, *The Theory of Stochastic Processes* (Chapman and Hall, London, 1965).
[36] H. E. Plesser, Ph.D. thesis, Göttingen, 1999.
[37] J. Franklin and W. Bair, SIAM (Soc. Ind. Appl. Math.) J. Appl. Math. **55**, 1074 (1995).
[38] J. G. Proakis and D. G. Manolakis, *Digital Signal Processing: Principles, Algorithms, and Applications* (Prentice-Hall, Englewood Cliffs, NJ, 1996).
[39] M. Stemmler, Network Comput. Neural Syst. **7**, 687 (1996).
[40] T. Shimokawa, A. Rogel, K. Pakdaman, and S. Sato, Phys. Rev. E **59**, 3461 (1999).
[41] A. Papoulis, *Probability, Random Variables, and Stochastic Processes*, 3rd ed. (McGraw-Hill International Editions, Singapore, 1991).
[42] W. A. Gardner, *Cyclostationarity in Communication and Sig-*

nal Processing (IEEE Press, New York, 1994).
[43] P. Amblard and S. Zozor, Phys. Rev. E **59**, 5009 (1999).
[44] H. L. Hurd, SIAM (Soc. Ind. Appl. Math.) J. Appl. Math. **26**, 203 (1974).
[45] M. H. Choi, R. F. Fox, and P. Jung, Phys. Rev. E **57**, 6335 (1998).
[46] C. C. Chow, T. T. Imhoff, and J. J. Collins, Chaos **8**, 616 (1998).
[47] A. Capurro, K. Pakdaman, T. Nomura, and S. Sato, Phys. Rev. E **58**, 4820 (1998).
[48] T. Kanamaru, T. Horita, and Y. Okabe, Phys. Lett. A **255**, 23 (1999).